

## ESR and magnetization in Jahn-Teller-distorted $\text{LaMnO}_{3+\delta}$ : Correlation with crystal structure

M. Tovar, G. Alejandro, A. Butera, A. Caneiro, M. T. Causa,\* F. Prado, and R. D. Sánchez  
*Centro Atómico Bariloche and Instituto Balseiro, Comisión Nacional de Energía Atómica and Universidad Nacional de Cuyo,*  
 8400 San Carlos de Bariloche, Río Negro, Argentina

(Received 21 January 1999)

We present magnetic susceptibility, x-ray-diffraction, and electron-spin-resonance (ESR) studies in the series of nonstoichiometric compounds  $\text{LaMnO}_{3+\delta}$ , for  $0 \leq \delta \leq 0.07$ . The measurements were performed in the paramagnetic regime, especially near the temperature  $T_{JT}$  for the Jahn-Teller transition observed in these samples. We observed important anomalies in both  $\chi_{dc}(T)$  and ESR linewidth  $\Delta H_{pp}(T)$  near  $T_{JT}$ , which was found dependent on  $\delta$ . We explain these observations considering the crucial role of the lattice distortions which strongly affect the magnetic interactions. For the ESR spectra we assume a spin Hamiltonian including single-ion crystal-field interaction as well as isotropic and Dzyaloshinskii-Moriya (DM) antisymmetric spin-spin exchange. We found that the Curie-Weiss temperature and the high- $T$  limit of the ESR linewidth, which are usually constant parameters, are in this case temperature dependent. We have been able to reproduce the behavior of  $\chi_{dc}(\delta, T)$  and  $\Delta H_{pp}(\delta, T)$ , including the anomalies at  $\approx T_{JT}$ , with a simple model where the  $T$  dependence of the exchange constants and of the crystal-field interaction are proportional to the orthorhombic strain. By contrast, the DM coefficient is constant for all  $\delta$  and  $T$  and would depend only on the tilting of the  $\text{MnO}_6$  octahedra which is approximately the same for all the samples studied. A structural and magnetic phase-diagram  $T$  versus  $\delta$  is also discussed. [S0163-1829(99)00738-9]

### I. INTRODUCTION

Lanthanum based mixed-valent manganites have received considerable attention in recent years due to their colossal magnetoresistance (CMR). The parent compound,  $\text{LaMnO}_3$ , is an insulating material that orders antiferromagnetically<sup>1,2</sup> (AFM) at  $T_N = 140$  K. Electron holes may be introduced by doping with divalent ions, such as  $\text{Ca}^{2+}$ ,  $\text{Sr}^{2+}$ , or  $\text{Ba}^{2+}$ . Then, some of the  $\text{Mn}^{3+}$  ions convert to  $\text{Mn}^{4+}$  and the double exchange mechanism becomes operative<sup>3</sup> giving rise to ferromagnetic (FM) interactions between the Mn ions, providing a metallic character to the material, and eventually CMR. On the other hand,  $\text{LaMnO}_3$  exhibits a wide range of oxidative nonstoichiometry<sup>4</sup> reflected in the general formula  $\text{LaMnO}_{3+\delta}$ . The excess oxygen ions cannot be accommodated in interstitial sites of the perovskite structure and the oxidation process is accomplished through the formation of cation vacancies (both of La and Mn).<sup>5</sup> Changes in  $\delta$  modify the ratio  $\text{Mn}^{3+}/\text{Mn}^{4+}$  and, as in the case of  $\text{La}_{1-x}\text{A}_x\text{MnO}_3$ , a FM metallic state can be achieved,<sup>4</sup> for which CMR has also been reported.<sup>6</sup>

$\text{LaMnO}_3$  crystallizes in the perovskite structure and its magnetic properties are strongly dependent on the lattice distortions which affect the magnetocrystalline anisotropy, as well as the isotropic and anisotropic exchange interactions.<sup>7,8</sup> At room temperature, the unit cell of  $\text{LaMnO}_3$  is orthorhombic, with a  $Pnma$  space group. In this case, the symmetry has been reduced from the ideal cubic perovskite by a tilting of the  $\text{MnO}_6$  octahedra. Superimposed to this distortion a pronounced cooperative Jahn Teller (JT) deformation is present<sup>9,10</sup> ( $O'$  phase). The JT distortion removes the degeneracy of the localized  $e_g$  electrons at the Mn sites and the occupied  $e_{g,\theta}$  orbitals are oriented alternately along the  $a$

and  $c$  crystal axes. This orbital ordering is essential for the  $A$ -type antiferromagnetism observed in neutron scattering experiments.<sup>11,12</sup> When  $\text{LaMnO}_3$  is heated to  $T_{JT} \approx 700\text{--}750$  K in Ar, the JT distortion disappears and the crystal symmetry becomes pseudocubic.<sup>9</sup> This is actually a  $Pnma$  structure ( $O$  phase), that preserves the tilting of almost undistorted oxygen octahedra.<sup>9</sup> Both phases have been found to coexist in a wide temperature range around  $T_{JT}$  giving rise to a hysteretic behavior<sup>13</sup> in the dc susceptibility  $\chi_{dc}$ . At  $T_R = 1010$  K a transition to a rhombohedral  $R\bar{3}c$  structure is observed.<sup>9</sup>

In the case of  $\text{LaMnO}_{3+\delta}$  the system evolves, as  $\delta$  increases, from the  $A$ -type antiferromagnetism observed for  $\delta = 0$  towards a ferromagnetic state, as indicated by magnetic measurements and neutron-scattering experiments.<sup>2</sup> In order to understand this process it is important to correlate the magnetic behavior with the structural changes that occur in the oxygenated compounds. In this paper, we present a detailed study of the magnetic and crystalline properties as a function of temperature in a series of  $\text{LaMnO}_{3+\delta}$  samples prepared with carefully controlled oxygen content. The behavior in the paramagnetic (PM) regime has been studied with particular emphasis in the neighborhood of the crystallographic transitions, especially near the JT transition. We followed the evolution of the JT distortion as a function of  $T$  for samples with different degrees of oxidation using x-ray-diffraction techniques and compared the behavior observed with the results of dc-magnetization measurements. In order to investigate the effects of the structural changes on the relaxation mechanisms active in different  $T$  regions, the electron-spin-resonance (ESR) spectra versus  $T$  was measured to probe the spin dynamics. We will show that ESR and  $\chi_{dc}$  results in the PM state can be explained in terms of a spin Hamiltonian, which includes crystal-field and ex-

TABLE I. Final firing conditions adopted for different oxygen compositions.

Oxygen composition ( $3 + \delta$ )	$P(\text{O}_2)$ in atm
3.00	$1.0 \times 10^{-5}$
3.03	$8.0 \times 10^{-3}$
3.04	$1.7 \times 10^{-2}$
3.05	$4.4 \times 10^{-2}$
3.07	$1.9 \times 10^{-1}$

change interactions, and whose coefficients are directly dependent on the strength of the orthorhombic strain.

## II. EXPERIMENT

### A. Sample preparation and experimental techniques

Ceramic polycrystalline samples of  $\text{LaMnO}_3$  were prepared by the nitrate method from high-purity oxides, as described in Ref. 13. Samples of  $\text{LaMnO}_{3+\delta}$  with different oxygen content ( $0 \leq \delta \leq 0.07$ ) were obtained through a final heat treatment at  $1000^\circ\text{C}$  in an appropriate oxygen/argon atmosphere with carefully controlled partial oxygen pressure,  $p(\text{O}_2)$ , followed by quenching to liquid-nitrogen temperature. In Table I we give the preparation conditions of our samples. Thermogravimetric analysis up to  $600^\circ\text{C}$  under a vacuum of 50 mTorr did not show any appreciable variation of the oxygen composition,  $3 \pm \delta$ , within an experimental uncertainty of  $\pm 0.003$ . The crystalline structure was studied by powder x-ray diffraction, between 300 and 950 K. For the studies at high temperature, the sample was spread on a resistively heated platinum ribbon mounted in an Anton Paar HTK-10 camera coupled to the diffractometer. In order to preserve the oxygen stoichiometry, the measurements were carried out under a vacuum of 20 mTorr. The diffractograms were obtained with a collection time of 10 s by step of  $0.02^\circ$  and the lattice parameters at each temperature were determined by the Rietveld method.

The magnetic susceptibility was measured from 100–950 K, using a superconducting quantum interference device magnetometer below room temperature and a Faraday balance magnetometer above it. The high-temperature measurements were made in vacuum and the sample mass was simultaneously monitored with the magnetometer balance. Changes in the sample mass during the experiments were less than 0.03%, an indication that the molar oxygen content remained constant within 0.005. The ESR experiments were performed at 9.5 GHz using a Bruker ESP-300 spectrometer from 100–770 K. The samples were measured in air and we have checked, using thermogravimetric techniques, that  $\delta$  does not change within the studied temperature range.

### B. Crystal structure

Our  $\text{LaMnO}_{3+\delta}$  samples present a  $Pnma$  orthorhombic structure at room temperature for all values of  $\delta$ . In Fig. 1 we show the temperature dependence of the cell parameters for three selected samples, with  $\delta=0, 0.03$ , and  $0.05$ . All the samples showed a tilting of the  $\text{MnO}_6$  octahedra of similar magnitude. At room temperature,  $\langle \varphi \rangle = 13.8^\circ, 12.0^\circ, 12.8^\circ, 13.4^\circ$ , and  $11.8^\circ$  for  $\delta=0, 0.03, 0.04, 0.05$ , and  $0.07$ , respec-

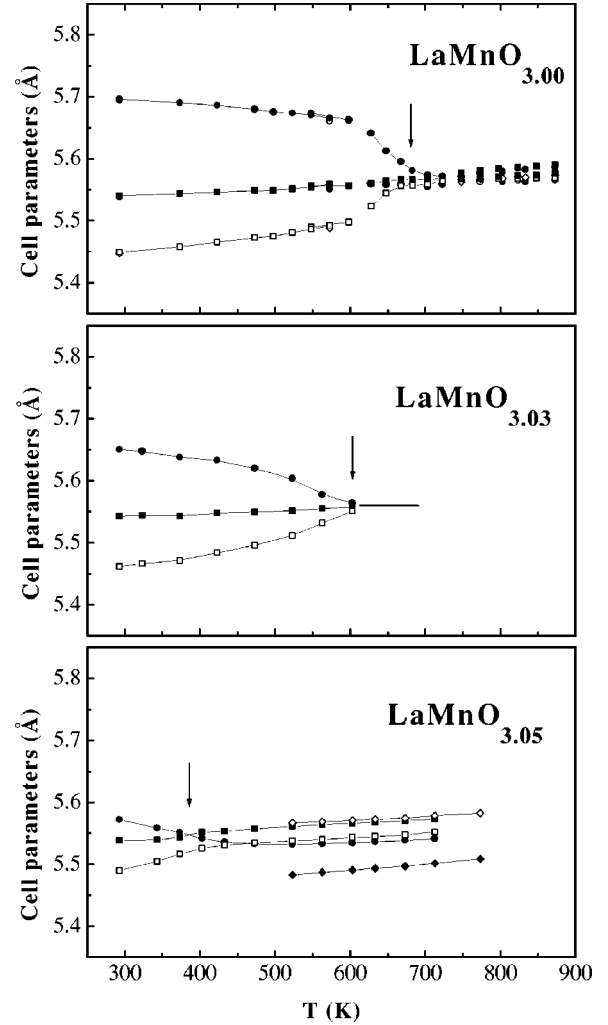


FIG. 1. Temperature dependence of the lattice parameters of  $\text{LaMnO}_{3+\delta}$  for three different values of  $\delta$ : circles correspond to  $a$  and squares to  $c$  (solid) and  $0.707b$  (open). Arrows indicate temperatures for Jahn-Teller transition. Data for  $\delta=0$  from Ref. 13 are included for comparison.

tively. Here, the average tilt  $\langle \varphi \rangle$  of  $\text{MnO}_6$  octahedra around the pseudocubic  $[111]$  direction was obtained from the two superexchange angles  $\theta_1 = \text{Mn-O}(1)\text{-Mn}$  and  $\theta_2 = \text{Mn-O}(2)\text{-Mn}$ . For  $\delta=0$  a pronounced cooperative Jahn Teller distortion in the  $ac$  plane is found ( $O'$  phase) at room temperature and, as  $T$  increases, the orthorhombic strain,  $s = 2(a-c)/(a+c)$ , diminishes monotonically, as discussed in detail in Ref. 13. Above  $725\text{ K}$ , only the pseudocubic  $O$  phase was present and  $T_{JT}$  was taken as the temperature where  $O$  and  $O'$  phases are present at 50%. In the temperature range of our experiments we did not observe the transition to the rhombohedral  $R\bar{3}c$  structure.<sup>4,9</sup> For  $\delta > 0$  we have found a significant reduction of the lattice distortion and a decrease of  $T_{JT}$ , as shown in Fig. 1. Since coexistence of the  $O$  and  $O'$  phases was not detected for the samples with  $\delta = 0.03$  and  $0.05$ , we defined  $T_{JT}$  as the temperature where  $s=0$ . For  $\delta=0.05$ , the  $R\bar{3}c$  structure was found to coexist with the  $O$  phase for an extensive temperature range, between 500 and 700 K. For the sample with  $\delta=0.07$ , the orthorhombic strain is close to zero at room temperature ( $a = 5.5397\text{ \AA}$ ,  $c = 5.5371\text{ \AA}$ ,  $b/\sqrt{2} = 5.5084\text{ \AA}$ ).

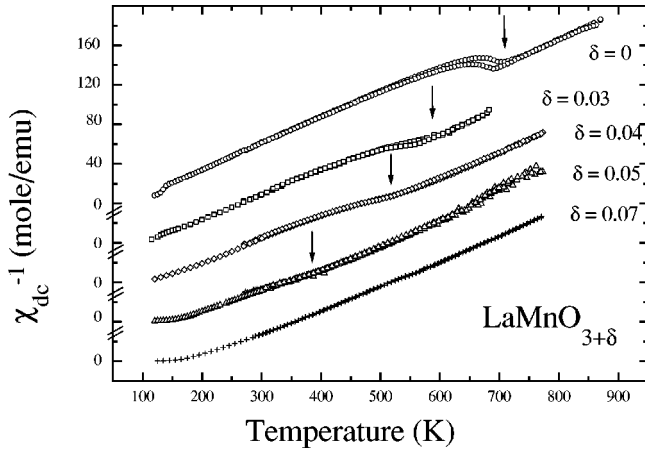


FIG. 2. Inverse of the susceptibility,  $\chi_{dc}^{-1}(T)$  vs  $T$ . Plots for different  $\delta$  values were displayed for clarity. Arrows indicate anomalies associated to JT transitions. Data for  $\delta=0$  from Ref. 8 are included for comparison.

### C. Magnetic susceptibility

The dc magnetic susceptibility shows two distinct regimes<sup>8</sup> for  $\text{LaMnO}_3$ , above and below  $T_{JT}$ . For  $T > T_{JT}$ , the susceptibility follows a ferromagnetic Curie-Weiss (CW) law,  $\chi_{dc}(T) = C/(T - \Theta)$ , with  $C = 3.6(2)$  emu K/mole and  $\Theta \cong 205(10)$  K. For  $T < T_{JT}$  deviations from linearity in  $\chi_{dc}^{-1}(T)$  were observed in agreement with the findings of Jonker<sup>14</sup> and, below  $T \approx 0.8T_{JT}$ , an almost linear behavior is recovered but with a strongly reduced CW temperature,  $\Theta \cong 75$  K. For the oxygenated samples with  $0 < \delta \leq 0.05$ , similar anomalies were observed at progressively lower temperatures, following the structural transformations reported in the previous section, as can be seen comparing Figs. 1 and 2. The Curie constant, as determined above  $T_{JT}$ , is approximately independent of  $\delta$ .

The deviations from linearity in  $\chi_{dc}^{-1}(T)$  may be interpreted in terms of a Curie-Weiss law where a continuous variation of  $\Theta$  with  $T$  is allowed because of the dependence of the exchange parameters with  $T$ , associated with the changes in the crystal structure. The values of  $\Theta(T)$  obtained for  $0 \leq \delta \leq 0.07$  are shown in Fig. 3(a). We observe that  $\Theta(T)$  is temperature independent in the  $O$  phase and shows only a moderate increase with  $\delta$ . Large variations in  $\Theta(T)$  are observed around  $T_{JT}$ , in coincidence with the major changes in the lattice parameters, and  $\Theta(T)$  approaches again a constant value at lower temperatures.

### D. ESR spectroscopy

As in the case of the stoichiometric compound<sup>8</sup> the ESR spectrum of  $\text{LaMnO}_{3+\delta}$  consists of a single line with Lorentzian shape and  $g = 1.98(1)$ , independent of oxygen concentration and temperature in the paramagnetic phase. The ESR double integrated intensity,  $I_{ESR}(T)$ , follows the temperature dependence of the dc magnetic susceptibility in the PM regime (see Fig. 4). At a given temperature  $I_{ESR}$  increases with  $\delta$  reflecting the strengthening of the FM interactions in oxygenated samples. For  $\text{LaMnO}_3$ , the  $I_{ESR}$  reaches a maximum value at  $T \approx 150$  K and shows a steep decrease to zero defining a Néel temperature,  $T_N = 137$  K. The loss of the ESR

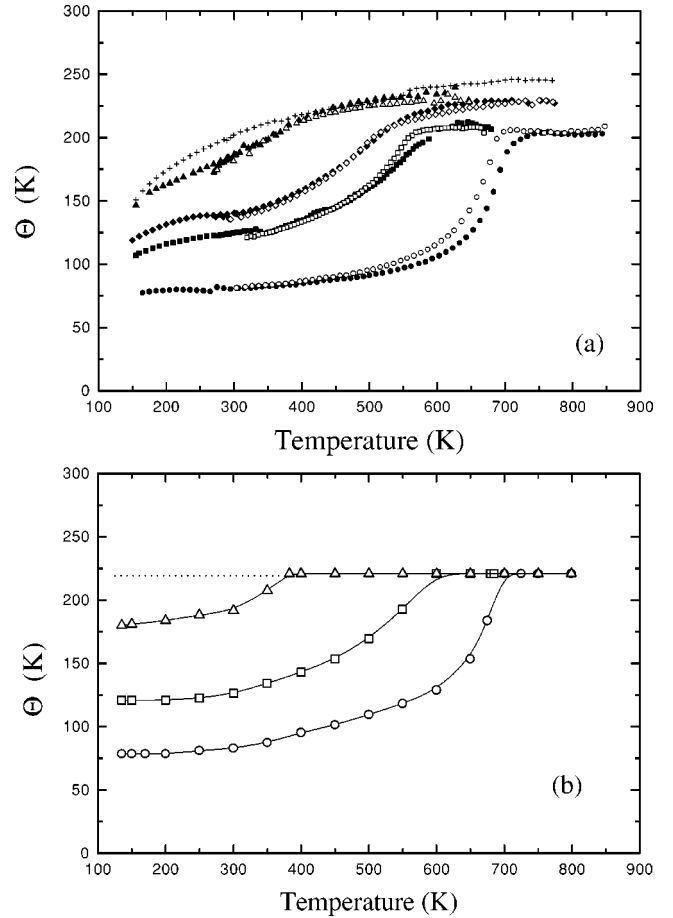


FIG. 3. Curie-Weiss temperature  $\Theta(T)$  vs  $T$  for different  $\delta$  values: (○)  $\delta=0$ , (□)  $\delta=0.03$ , (◇)  $\delta=0.04$ , (△)  $\delta=0.05$ , and (+)  $\delta=0.07$ . Open (solid) symbols correspond to increasing (decreasing) temperature. (a) Experimental data obtained from  $\chi_{dc}(\delta, T)$ . (b)  $\Theta(T)$  calculated using Eqs. (3.3) and (3.4). For simplicity we have taken an average value for  $J(T > T_{JT})$ .

signal in the antiferromagnetic phase is due to the presence of an energy gap  $\Delta E_g$  in the resonance modes spectrum. Antiferromagnetic resonance (AFMR) experiments<sup>15</sup> at much higher frequencies (100–700 GHz) have shown that  $\Delta E_g/k_B \cong 25$  K. For  $\text{LaMnO}_{3.03}$ , the behavior of the ESR intensity is similar, although with an increased intensity and a small shift of the anomalies towards lower temperatures ( $T_N = 128$  K). Instead, for the more oxygenated samples,  $I_{ESR}$  continues to increase through the transition temperature as shown in the inset of Fig. 4. This behavior indicates the suppression of the AF gap and is in agreement with the observation of FM peaks in neutron-scattering experiments<sup>2</sup> for  $\delta > 0.025$ .

The  $T$  dependence of the ESR linewidth,  $\Delta H_{pp}(T)$ , is shown in Fig. 5 for the PM regime. Near the ordering temperature a fast broadening is observed in all cases, associated with the magnetic transition.<sup>16,17</sup> As  $T$  increases,  $\Delta H_{pp}$  goes through a minimum value at about  $T_{min} \approx 180$  K. For  $\delta = 0.07$ ,  $\Delta H_{pp}(T)$  increases monotonically above  $T_{min}$ , in coincidence with the dependence found in the doped CMR ferromagnetic manganites<sup>16</sup>  $\text{La}_{0.67}(\text{Ca}, \text{Sr}, \text{Pb})_{0.33}\text{MnO}_3$ . For  $\delta \leq 0.05$  the behavior is more complex and two temperature regions may be identified, above and below  $T_{JT}$ . For  $T > T_{JT}$ , the linewidth is independent of  $\delta$ . Instead, for  $T$

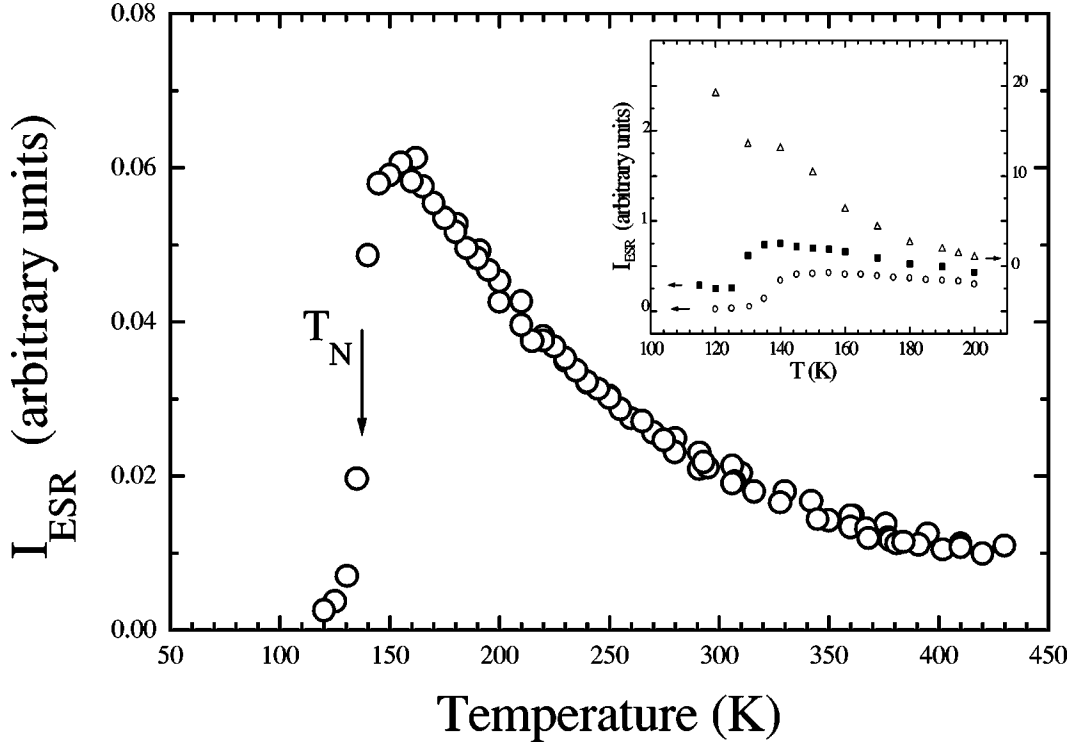


FIG. 4. ESR double integrated intensity,  $I_{ESR}$  vs  $T$  for  $\delta=0$ . Inset: idem for 0.03 ( $\square$ ), and 0.05 ( $\triangle$ ).

$\langle T_{JT} \rangle$ , a strong dependence of  $\Delta H_{pp}(T)$  with  $\delta$  is observed, with a significant increase that correlates with the JT distortion in the  $O'$  phase.

### III. DISCUSSION

#### A. Isotropic exchange interaction and CW temperatures

The magnetic properties of insulating perovskites are mainly controlled by the isotropic superexchange interactions between localized Mn ions. For the stoichiometric compound  $\text{LaMnO}_3$  neutron-diffraction experiments<sup>11</sup> have shown that in the JT distorted  $O'$  phase,  $A$ -type antiferromagnetic ordering occurs below  $T_N$ . This kind of magnetic order arises from ferromagnetic interactions within the  $ac$  planes and antiferromagnetic interplane coupling. For the isotropic Heisenberg Hamiltonian

$$\mathcal{H}_{ex} = -2 \sum_{i < j} J_{ij} \vec{S}_i \vec{S}_j \quad (3.1)$$

the constant  $J_{ij} = J_{ac}$  describes the FM in-plane exchange and  $J_{ij} = J_b$  the interplane AFM coupling. Values for  $J_{ac}$  and  $J_b$  may be estimated from the measured  $T_N$  and  $\Theta$  using the Weiss mean-field equations:

$$T_N = (4/3)S(S+1)(2J_{ac} - J_b)/k_B \quad (3.2)$$

and

$$\Theta = (4/3)S(S+1)(2J_{ac} + J_b)/k_B, \quad (3.3)$$

where  $J_{ac} = J_{ac}^{(1)} + J_{ac}^{(2)}$  and  $J_b = J_b^{(1)} + 4J_b^{(2)}$ . The superscripts (1) and (2) indicate the coupling between first- and second-nearest neighbors.<sup>7</sup> Since the exchange parameters are ex-

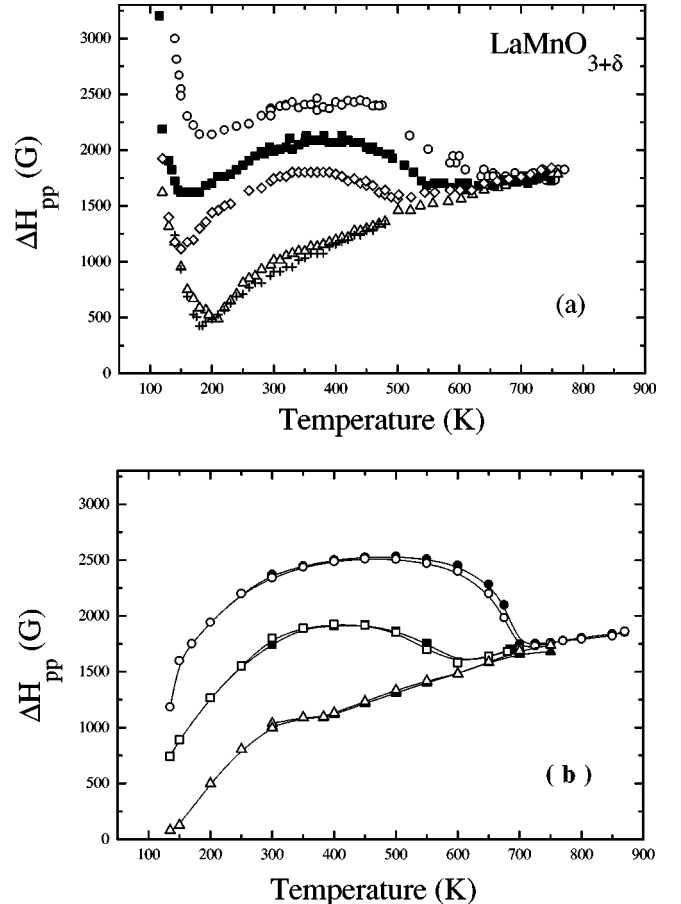


FIG. 5. ESR linewidth vs  $T$  for different studied samples: ( $\circ$ )  $\delta=0$ , ( $\square$ )  $\delta=0.03$ , ( $\diamond$ )  $\delta=0.04$ , ( $\triangle$ )  $\delta=0.05$ , and ( $+$ )  $\delta=0.07$ . (a) Experimental data. (b) Calculated from Eqs. (3.5) and (3.9).

pected to vary with  $T$  as a consequence of changes in the crystal structure,  $\Theta$  will be  $T$  dependent.

In the pseudocubic  $O$  phase the octahedral symmetry of the Mn-O-Mn bonds indicates that  $J_{ac}=J_b$ . From the constant value of  $\Theta$  measured above  $T_{JT}$ ,  $J_{ac}/k_B=J_b/k_B=8.5(8)$  K is obtained in the case  $\delta=0$ . For  $T$  close to  $T_N$ , where  $\Theta(T)$  is again approximately constant, we derived from Eqs. (3.2) and (3.3):  $J_{ac}/k_B=6.7(4)$  K and  $J_b/k_B=-3.7(8)$  K. The changes observed between the  $O$  and the  $O'$  phases are in qualitative agreement with theoretical estimates based on local spin-density approximation.<sup>7,18</sup> These calculations predict an isotropic FM value,  $J_{ac}=J_b$ , in the pseudocubic  $O$  phase. When the lattice presents a JT distortion, a decrease in the magnitude of both exchange constants is expected and the calculations<sup>7</sup> show that  $J_{ac}$  remains FM while  $J_b$  changes to AFM in the distorted  $O'$  phase. As seen in Fig. 3(a), the largest variations in  $\Theta(T)$ , and consequently in the estimates of  $J_{ij}(T)$ , are observed around  $T_{JT}$ .

For the oxygenated samples Fig. 3(a) shows that the variation of  $\Theta(T)$  below  $T_{JT}$  is significantly reduced in comparison with the case of  $\delta=0$ , reflecting qualitatively the smaller JT distortions (see Fig. 1). A quantitative relation can be established assuming that the dependence of  $J_{ij}$  on  $\delta$  and its variation with  $T$  are both proportional to the JT distortion through the orthorhombic strain parameter  $s(\delta, T)$ . Assigning the value  $J^O=J_{ij}(\delta=0; T>T_{JT})$  to the pseudocubic lattice ( $s=0$ ) and the value  $J_{ij}^{O'}=J_{ij}(\delta=0; T\cong T_N)$  to  $s_0=0.029$  extrapolated to  $T_N$  for our sample of  $\delta=0$ , we assume:

$$J_{ij}(\delta, T) = J^O + (J_{ij}^{O'} - J^O)s(\delta, T)/s_0. \quad (3.4)$$

Using this equation and the measured orthorhombic strains  $s(\delta, T)$  we have calculated  $\Theta(T)$  for  $\delta=0, 0.03$ , and  $0.05$ , shown in Fig. 3(b). A comparison with the experimental results of Fig. 3(a) shows an excellent agreement. With the values calculated in this way for  $J_{ij}(\delta, T)$ , we have also calculated the ordering temperature for  $\text{LaMnO}_{3.03}$  using Eq. (3.2), and obtained  $T_N=129$  K, in coincidence with the ESR result shown in the inset of Fig. 4. For  $\delta\geq 0.05$ , Eq. (3.4) predicts that both  $J_{ac}$  and  $J_b$  are positive. Then the interplane order should disappear and the materials become FM. This behavior is in agreement with neutron scattering results<sup>2</sup> and the observed dependence of  $I_{ESR}(T)$ . In these cases the expected mean-field FM ordering temperature is  $T_C=\Theta$ . For  $\text{LaMnO}_{3.05}$  the calculated ordering temperature increases to 195 K.

For  $\delta=0.07$  we observed a positive curvature (see Fig. 2) for  $\chi_{ac}^{-1}(T)$  versus  $T$  in the whole temperature range, characteristic of the ferromagnetic CMR manganites. This behavior is due to short-range order and has been described in terms of the constant coupling approximation in Ref. 16. Because of it, an apparent reduction of  $\Theta(T)$  is observed near the magnetic transition temperature with a negative curvature of  $\Theta(T)$  vs  $T$ , deviating from the mean-field behavior implicit in Fig. 3(b). Similar effects are observed in Fig. 3(a) for all values of  $\delta$  below  $\approx 250$  K.

### B. Anisotropic interactions and ESR linewidths

As discussed in Ref. 16 the temperature dependence of the ESR linewidth can be expressed by

$$\Delta H_{pp}(T) = [C/T\chi_{dc}(T)]\Delta H_{pp}^{\infty}, \quad (3.5)$$

where  $\Delta H_{pp}^{\infty}$  is identified with the high-temperature limit of the linewidth and may be used as an adjustable parameter to fit the experimental data. In magnetic insulators with large exchange interactions,  $\Delta H_{pp}^{\infty}$  is usually described by exchange narrowing models. Here, the linewidth is proportional to  $\omega_p^2/\omega_e$ , where  $\omega_e$  is the frequency associated with isotropic exchange and  $\omega_p$  includes the contributions due to anisotropic interactions. The classical dipolar interaction is commonly the source of linewidth broadening which accounts for  $\omega_p$ , but in the perovskite manganites its contribution to  $\Delta H_{pp}^{\infty}$  is only of a few Gauss.<sup>19</sup> Thus other contributions should be considered, particularly those expected to be sensitive to the structural changes. We include in this work crystal-field (CF) and antisymmetric exchange terms arising from Dzyaloshinskii-Moriya (DM) interactions.<sup>20</sup>

In the case of the JT distorted  $\text{LaMnO}_{3+\delta}$  a series of octahedra elongated alternately along the  $a$  and  $c$  axes (orbital ordering) constitutes a good description<sup>12</sup> of the lattice below  $T_{JT}$ . Then, the crystal-field interaction may be described by an effective spin Hamiltonian ( $S=2$  for  $\text{Mn}^{3+}$  ions),

$$\mathcal{H}_{CF} = -D \sum_{i=1}^{N/2} S_{x(i)}^2 - D \sum_{j=1}^{N/2} S_{z(j)}^2, \quad (3.6)$$

where  $i$  and  $j$  represent alternate sites in the  $(ac)$  planes. For the quasicubic local environment of Mn ions found for the high-temperature  $O$  phase<sup>9</sup> no crystal-field contribution is expected in this second-order Hamiltonian.

Antisymmetric contributions to the superexchange interaction between Mn ions are allowed when the oxygen ions that mediate the interaction occupy crystal sites without inversion symmetry. The tilting of the oxygen octahedra found in most perovskites shifts the oxygen ions away from the  $\langle 100 \rangle$  axes, giving rise to a DM coupling between the Mn ions. The JT distortions within the  $(ac)$  planes may result in additional contributions to the DM interaction in the  $O'$  phase.<sup>21</sup> The Hamiltonian for this interaction is

$$\mathcal{H}_{DM} = \vec{D}_{jk}(\vec{S}_j \times \vec{S}_k). \quad (3.7)$$

The ESR linewidth is given, in the high-temperature approximation, by

$$\Delta H_{pp}^{\infty} = (2/\sqrt{3})(\hbar/g\mu_B)(1/T_2) = (\sqrt{2\pi/3}/g\mu_B)(M_2^{3/2}/M_4^{1/2}), \quad (3.8)$$

where  $M_2$  and  $M_4$  are the second and fourth moments of the spectral distribution, respectively. As described in Ref. 21 a general expression for  $\Delta H_{pp}^{\infty}$ , valid for all the studied compounds well above  $T_N$ , is

$$\Delta H_{pp}^{\infty} = \frac{(\sqrt{2\pi/3})(2.8D^2 + 21.3D^2)^{3/2}}{g\mu_B(806D^2\langle J^2 \rangle + 825D^2\langle\langle J^2 \rangle\rangle)^{1/2}}, \quad (3.9)$$

where  $\langle J^2 \rangle = (2J_{ac}^2 + J_b^2)/3$  and  $\langle\langle J^2 \rangle\rangle = (310J_{ac}^2 + 114J_b^2 + 40J_{ac}J_b)/464$ . This expression includes two adjustable parameters for the anisotropic interactions, which are intimately related to the local environment of the Mn ions and

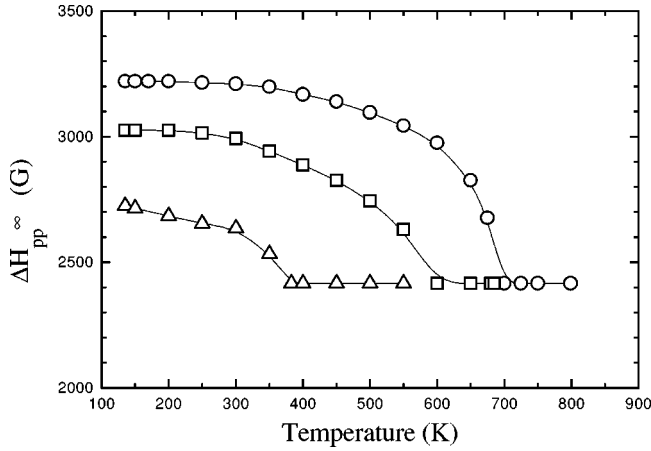


FIG. 6. Evaluation of the  $T$  dependence of  $\Delta H_{pp}^{\infty}$  from Eq. (3.9) as explained in the text. The calculation were performed for  $\delta=0$  ( $\circ$ ), 0.03 ( $\square$ ), and 0.05 ( $\triangle$ ).

should reflect the changes associated with the JT distortion. Thus both  $D$  and  $\mathcal{D}$  are expected to be temperature dependent and so is  $\Delta H_{pp}^{\infty}$ .

From the experimental values for  $\Delta H_{pp}(T)$ , and using the measured  $\chi_{dc}(T)$  to calculate the prefactor in Eq. (3.5), we have determined  $\Delta H_{pp}^{\infty}$  at different temperatures. For the pseudocubic  $O$  phase we obtained a constant value,  $\Delta H_{pp}^{\infty} = 2415$  G, independent of  $\delta$ . Assuming  $D=0$  in Eq. (3.9) and  $\langle\langle J^2 \rangle\rangle^{1/2} \cong J^O$ , as derived from  $\Theta(T)$  for  $T > T_{JT}$ , we found  $\mathcal{D}/k_B = 0.78$  K. In this phase, the DM interaction is related to the tilting of the octahedra that is almost constant<sup>9</sup> with  $T$ , and we have found it to change very little with  $\delta$ .

In the  $O'$  phase the CF interaction cannot be neglected. Moussa *et al.*<sup>1</sup> have estimated  $\mathcal{D}/k_B = 1.92$  K for  $\text{LaMnO}_3$  at 1.4 K from neutron-scattering experiments and, since the magnitude of the crystal-field interaction is directly dependent on the JT distortion, we have assumed  $D$  to be proportional to the orthorhombic strain  $s(\delta, T)$ . We used a value  $D(\delta, T)/k_B = 1.92 K s(\delta, T)/0.038$  in Eq. (3.9), normalizing the CF contribution to the orthorhombic strain measured in Ref. 1. We further assumed that the exchange constants vary according to Eq. (3.4). Under these conditions, we have calculated the variation of  $\Delta H_{pp}^{\infty}$  with  $T$ , using different values for  $\mathcal{D}$  in Eq. (3.9). The best fitting to the data was obtained for  $\mathcal{D}/k_B = 0.8$  K almost coincident with the value derived for the  $O$  phase. The results of this calculation are given in Fig. 6, that clearly shows the dependence of  $\Delta H_{pp}^{\infty}$  with  $T$  and  $\delta$ . When the calculated  $\Delta H_{pp}^{\infty}$  is replaced in Eq. (3.5), an excellent agreement with the experimental data for  $\Delta H_{pp}(T)$  is obtained, as seen in Fig. 5. As  $\mathcal{D}$  remains approximately constant through the JT transition, we conclude that the main contribution to the antisymmetric exchange originates in the tilting of the octahedra, that is essentially the same in both  $O$  and  $O'$  phases.<sup>9</sup>

### C. Structural and magnetic phase diagram

The results obtained in this work are summarized in the phase diagram ( $T$  vs  $\delta$ ) shown in Fig. 7. The JT transition temperature decreases monotonically as  $\delta$  increases, not being observed above room temperature for  $\delta=0.07$ . Notice in

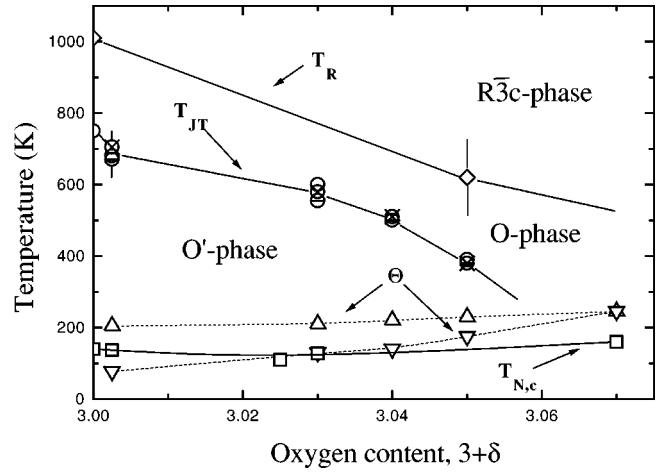


FIG. 7. Phase diagram  $T$  vs oxygen content. ( $\diamond$ ) indicates the  $Pnma$ - $R\bar{3}c$  transition temperature  $T_R$ . Circles indicate the Jahn Teller transition temperature,  $T_{JT}$  as determined from x-ray-diffraction ( $\circ$ ), ESR ( $\odot$ ), and dc susceptibility ( $\otimes$ ) data. The vertical lines indicate a two-phase field. Triangles indicate CW temperatures,  $\Theta$ : ( $\triangle$ ) and ( $\nabla$ ) correspond to  $O$  and  $O'$  phases, respectively. ( $\square$ ) indicates the magnetic transition temperature  $T_N$  or  $T_c$ . We have included neutron-diffraction data:  $T_{JT}$  for  $\delta=0$  from Ref. 9 and  $T_{N,c}$  for  $\delta=0, 0.025$ , and  $0.07$  from Ref. 2.  $T_R$  for  $\delta=0$  determined by DTA in Ref. 9 is also shown. For clarity we have displayed our data within the experimental uncertainty for the oxygen content.

Fig. 1 that the orthorhombic strain decreases simultaneously with  $T_{JT}$ . Anomalies in the  $\chi_{dc}(T)$  and  $\Delta H_{pp}(T)$  are clearly associated with the structural JT transition. The temperatures where these anomalies are observed decrease with  $\delta$  following the  $T_{JT}$  behavior. On the contrary, we have not observed changes in the magnetic behavior at the orthorhombic-rhombohedral transition temperature  $T_R$ . The CW temperature for the  $O$  phase remains almost constant, varying from  $\Theta = 205$  K for  $\delta=0$  to  $\Theta = 245$  K for  $\delta=0.07$ . Instead, the values of  $\Theta$  derived for the JT distorted  $O'$  phase are much smaller, especially for  $\delta=0$ . As  $\delta$  increases and the orthorhombic strain decreases, the CW temperatures for both  $O$  and  $O'$  phases approaches a common value. For the samples with low oxygen content, the AFM ordering temperatures are larger than  $\Theta$ , reflecting the competition between the FM in-plane and the AFM interplane interactions, see Eqs. (3.2) and (3.3). For  $\delta=0.07$  the  $\chi_{dc}^{-1}(T)$  has the characteristic behavior of a FM manganite, with  $T_c = 165$  K (see Ref. 2), that is smaller than  $\Theta$  due to short-range order, as discussed in Ref. 16.

## IV. SUMMARY

We have analyzed the correlation between the structural and magnetic properties of  $\text{LaMnO}_{3+\delta}$  for the nonstoichiometry range  $0 \leq \delta \leq 0.07$ . We have found a direct dependence on the magnitude of the JT distortion for the variations with  $\delta$  and  $T$  of the dc susceptibility and the ESR linewidths. Because of the important structural changes observed as a function of  $T$ , two usually constant parameters become temperature dependent: the CW temperature,  $\Theta$ , and the linewidth in the high-temperature regime  $\Delta H_{pp}^{\infty}$ . We have been

able to reproduce the temperature dependence of  $\chi_{dc}(T)$ , including the anomalies at  $T \cong T_{JT}$ , with a simple model where the variations of the exchange constants were assumed to be linear in the orthorhombic strain  $s(\delta, T)$ . The behavior of  $\Delta H_{pp}^\infty$  was well described within this model including a second-order crystal-field Hamiltonian with a parameter  $D(T, \delta)$  also proportional to  $s(\delta, T)$ . Its absolute magnitude was normalized to the experimental value determined from neutron-scattering experiments<sup>1</sup> for  $\delta=0$  and  $T=1.4$  K. A single additional parameter describing the DM interaction,  $D/k_B \cong 0.8$  K, was necessary to explain the ESR data. This parameter was found to be essentially the same for both the  $O$  and  $O'$  phases, constant with  $T$ , and independent of  $\delta$ . Thus we conclude that this interaction is mainly related to the tilting of the  $\text{MnO}_6$  octahedra, that preserves its magnitude through the JT transition. Finally, since the JT distortion

becomes smaller with the increase of the oxygen content, the  $A$  type antiferromagnetism associated with the JT orbital ordering tends to disappear. Simultaneously, the system becomes ferromagnetic and both the dc susceptibility and the ESR spectra show the characteristic behavior found in CMR manganites.

#### ACKNOWLEDGMENTS

We like to thank S. B. Oseroff for helpful comments and critical reading of the manuscript and M. Vásquez-Mansilla for assistance with the Faraday balance experiments. We acknowledge partial support of EEC (Commission DGXII, Contract No. GCI1\*C792-0087) and CONICET-Argentina (LANAIS 34 and PID 4947). G.A. acknowledges support from Ministerio de Educación-FOMEC (Argentina).

\*Electronic address: causa@cab.cnea.gov.ar

- <sup>1</sup>F. Moussa, M. Hennion, J. Rodríguez Carvajal, A. H. Mouden, L. Pinsard, and A. Revcolevschi, *Phys. Rev. B* **54**, 15 149 (1996).
- <sup>2</sup>C. Ritter, M. R. Ibarra, J. M. De Teresa, P. A. Algarabel, C. Marquina, J. Blasco, J. García, S. Oseroff, and S-W. Cheong, *Phys. Rev. B* **56**, 8902 (1997).
- <sup>3</sup>C. Zener, *Phys. Rev.* **82**, 403 (1951).
- <sup>4</sup>J. Töpfer and J. B. Goodenough, *J. Solid State Chem.* **130**, 117 (1997).
- <sup>5</sup>J. A. M. van Roosmalen and E. H. P. Cordfunke, *J. Solid State Chem.* **110**, 109 (1994).
- <sup>6</sup>R. Mahendiran, S. K. Tiwary, A. K. Raychaudhuri, T. V. Ramakrishnan, R. Mahesh, N. Rangavittal, and C. N. R. Rao, *Phys. Rev. B* **53**, 3348 (1995).
- <sup>7</sup>I. Solovyev, N. Hamada, and K. Terakura, *Phys. Rev. Lett.* **76**, 4825 (1996).
- <sup>8</sup>M. T. Causa, G. Alejandro, R. Zysler, F. Prado, A. Caneiro, and M. Tovar, *J. Magn. Magn. Mater.* **196-197**, 506 (1999).
- <sup>9</sup>J. Rodríguez Carvajal, M. Hennion, F. Moussa, A. H. Mouden, L. Pinsard, and A. Revcolevschi, *Phys. Rev. B* **57**, R3189 (1998).
- <sup>10</sup>Q. Huang, A. Santoro, J. W. Lynn, R. W. Erwin, J. A. Borchers, J. L. Peng, and R. L. Greene, *Phys. Rev. B* **55**, 14 987 (1997).
- <sup>11</sup>E. O. Wollan and W. C. Koehler, *Phys. Rev.* **100**, 545 (1955).
- <sup>12</sup>J. B. Goodenough, *Magnetism and the Chemical Bond* (Inter-

science Publishers, New York, 1963).

- <sup>13</sup>F. Prado, R. Zysler, L. Morales, A. Caneiro, M. Tovar, and M. T. Causa, *J. Magn. Magn. Mater.* **196-197**, 481 (1999).
- <sup>14</sup>G. H. Jonker, *Physica (Amsterdam)* **22**, 707 (1956).
- <sup>15</sup>S. Mitsudo, K. Hirano, H. Nojiri, M. Motokawa, K. Hirota, A. Nishizawa, N. Kaneko, Y. Endoh, *J. Magn. Magn. Mater.* **177-181**, 877 (1998).
- <sup>16</sup>M. T. Causa, M. Tovar, A. Caneiro, F. Prado, G. Ibañez, C. A. Ramos, A. Butera, B. Alascio, X. Obradors, S. Piñol, F. Rivadulla, C. Vázquez-Vázquez, M. A. López-Quiutela, J. Rivas, Y. Tokura, and S. B. Oseroff, *Phys. Rev. B* **58**, 3233 (1998).
- <sup>17</sup>M. Domínguez, S. E. Lofland, S. M. Baghat, A. K. Raychaudhuri, H. L. Ju, T. Venkatesan, and R. L. Greene, *Solid State Commun.* **97**, 193 (1996); S. E. Lofland, P. Kim, P. Dahiroc, S. M. Baghat, S. D. Tyagi, S. G. Karabashev, D. A. Shulyatev, A. A. Arsenov, and Y. Mukovskii, *Phys. Lett. A* **233**, 476 (1997).
- <sup>18</sup>I. Solovyev, N. Hamada, and K. Terakura, *Phys. Rev. B* **53**, 7158 (1996).
- <sup>19</sup>D. L. Huber, *J. Appl. Phys.* **83**, 6949 (1998).
- <sup>20</sup>I. Dzialoshinsky, *J. Phys. Chem. Solids* **4**, 241 (1958); T. Moriya, *Phys. Rev. Lett.* **4**, 228 (1960); *Phys. Rev.* **120**, 91 (1960).
- <sup>21</sup>D. L. Huber, G. Alejandro, A. Caneiro, M. T. Causa, F. Prado, M. Tovar, and S. B. Oseroff, *Phys. Rev. B* (to be published 1 November 1999).